



Corrosion protection studies of stainless steel alloy in hydrochloric acid by using electropolymerized poly (N-imidazolyl tetrahydrophthalamic acid)

Mayasa I.Ali^{1*}, Khulood A.Saleh¹

¹ Chemistry department, College of science, Baghdad University, Baghdad, Iraq

*Corresponding author E-mail: chemistmayasa@gmail.com

Abstract

The present work reports the electrochemical synthesis of poly (N-imidazolyl tetra hydro phthalamic acid) (PIP) from monomer (N-imidazolyl tetra hydro phthalamic acid) (NIP) in aqueous solution on surface of stainless steel (working electrode) by using electrochemical polymerization technique. The corrosion protection test for coated and uncoated stainless steel (SS) by polymer was studied in 0.2 M HCl solution by followed Tafel and Potentiostatic procedures. The structure of PIP was characterized by Fourier Transform Infrared (FTIR) spectroscopy and Atomic Force Microscope (AFM). Parameters of corrosion that include corrosion current density (icorr), corrosion potential (Ecorr) and protection efficiency (PE %) were studied. The effect of temperature in the range (293-323) K on the protection efficiency of coated and uncoated stainless steel also was studied. Polymer was modified by adding nanomaterials (Zinc Oxide (normal) (ZnO) and reduced graphene oxide (rGO)) into monomer solution to improve protection efficiency. The results obtained shown higher protection efficiency at 293 K. Kinetic and thermodynamic of activation parameters were studied for corrosion process for coated and uncoated stainless steel in acidic medium.

Keywords: Electrochemical Polymerization; Poly (N-Imidazolyl Tetrahydro Phthalamic Acid); Anticorrosion; Reduced Graphene Oxide; Stainless Steel Alloy.

1. Introduction

Conducting polymers as protecting from corrosion is one of the fields which have interests in recent years in coating science. Conducting polymer poly (N-imidazolyl tetrahydro phthalamic acid) or PIP was produced from electrochemical polymerization that involved electrodeposition of polymers on S.S that acting as working electrode. Monomer was dissolved in organic solvent and anodically polymerized on the electrode surface from the solution containing the monomer [1]. In general conducting polymers were organic compounds that have π orbital system and conjugated system along their polymer backbone, hence giving them unique optical and electrical properties because the conducting polymer combine the electrical properties of metals with the advantage of polymers such as light weight, workability and resistance to corrosion [2]. Therefore conducting polymers have many applications in variable fields that involves chemical sensors [3] (e.g. biosensor) [4, 5], molecular electronic devices (e.g. diodes and field effect transistors) [6], batteries [7], biomedical engineering [8], corrosion inhibitors [9-10], electrochromic devices [11], [12], supercapacitors [13], [14], electroluminescence [15], photovoltaic cells [16], [17], dye sensitized solar cells (DSSCs) [18], biofuel cells [14] or as drug delivery [19- 21] Graphene was added to conducting polymers to improve their properties due to its unique properties that involve high electrical conductivity, high thermal conductivity, tensile strength and large surface area [22]. Graphene-polymer composites based materials found wide applications in corrosion

protective coating applications [23-27]. The PIP/ Graphene mixture was then deposited on SS surface. In this paper the PIP and PIP/Graphene film were characterized by (FTIR) and (AFM). The corrosion parameters of SS in 0.2 M of HCl were studied by electrochemical polarization technique at temperature range (293-323K). The effect of coating film as anticorrosion was studied in absence and presence nanomaterials (rGO and ZnO).

2. Experimental

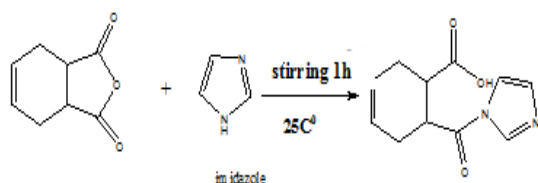
2.1. Reduced graphene oxide (rGO) was prepared by two steps

First step preparation of graphene oxide by using Hummers method [28]. In this method 1g of graphite powder was added into the (23 ml) concentrated sulfuric acid (in an ice bath) followed by the slowly addition of (0.5) g of sodium nitrate and (3g) of KMnO_4 and gradually with temperature near 2°C . Then mixture transferred into water bath at temperature 35°C and stirred for 15 min at 90°C , and then a thick phase was formed. After that (70 ml) of deionized water was added and followed by slowly addition (5 ml) of H_2O_2 to reduction of KMnO_4 . This addition turns the color of the paste to the light brown, then the paste washed by 5% HCl (85 ml) and after that the product was washed by deionized water until pH reached 6, finally the resultant product was filtered and dried. Second step chemical reduction of GO into reduced graphene oxide [28]. In this process (0.9 g) of GO was dispersed into (300

ml) deionized water, then was used ultrasonic for 1h to dispersed it. Then (10 ml) of hydrazine hydrate ($N_2H_4 \cdot H_2O$) was added and the solution was heated for 24h at $100^\circ C$. At the end, solution color changed from brown to the black. The product kept to cool, then filtered and washed by methanol and deionized water and dried at $50^\circ C$ for 6h.

2.2. Preparation of monomer (N-Imidazolyltetrahydro phthalamic acid) (NIP)

(2.235 g) of tetrahydro phthalic anhydride was dissolved in (10ml) of dioxane in round bottom flask at room temperature, then (1g) of imidazole was dissolved and added to the flask reaction and the reaction continued with stirring for 1h at $25^\circ C$. Finally white precipitate was formed, filtered and dried in vacuum, the reaction shown in scheme 1.



Scheme 1: Preparation of (N-imidazolyl tetrahydro phthalamic acid).

2.3. Electrochemical polymerization of (N-imidazolyl tetrahydro phthalamic acid) (NIP)

Electrochemical polymerization of NIP was occurred on S.S (working electrode) surface by using DC power supply. The electrode was polished by abrasive paper (2000 mesh) and washing by deionized water and acetone. Preparation solution for electropolymerization that involved dissolving (0.1g) monomer (NIP) in 100 ml of H_2O with three drops of conc. H_2SO_4 (95%), the polymer

film was deposited on anode electrode surface at 293K [29]. In addition nanomaterials that involved rGO (0.004 g) was mixed with monomer solution after dispersion it and also, ZnO_n (0.05) g was added into monomer solution to increase corrosion protection efficiency for coating film.

2.4. Electrochemical corrosion measurement

The corrosion cell was conducted with the use of advanced potentiostat, with all accessories, cell, electrode, and working electrode holder. The polarization curves were scanned between (-200) to (+200) mv from the open circuit potential and the corrosion currents i_{corr} , and corrosion potentials E_{corr} were evaluated by extrapolation of the cathodic and anodic Tafel lines for the polarization curves at four different temperatures. The corrosion measurements for S.S were studied in 0.2 M HCl solution at temperature range (293-323K).

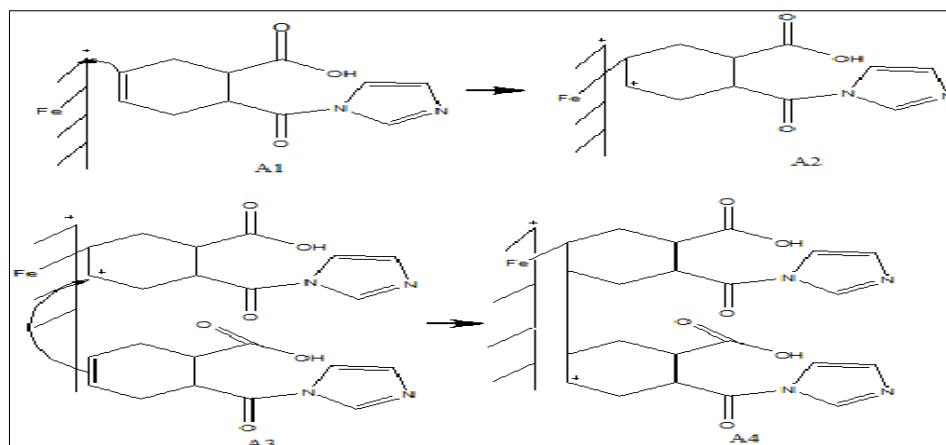
3. Results and discussion

3.1. Mechanism of polymerization

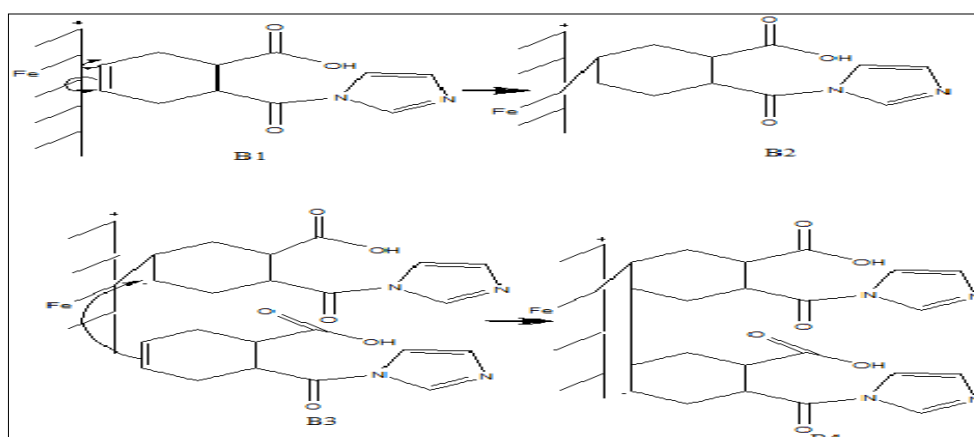
The Electropolymerization reactions were occurred according to cationic mechanism [30-36] and radical mechanisms in particular and growth of the PIP film on metal surface.

Cationic mechanism (Scheme 2-A):

First, transfer of electron from the monomer to the metal (working electrode). This transfer was led to formation radical cation which was adsorbed on metal surface shown in structure (A2). Those radical cation can desorbed and reacted in solution for giving rise into compound of low molecular weight (A3), then NIP monomer was added on via cationic mechanism at the charged end of the desorbed oxidized NIP (A4).



Scheme (2-A): Cationic Mechanism for Growth for PIP Film.



Scheme (2-B): Radical Mechanism for Growth PIP Film.

Radical mechanism (Scheme 2-B):

Radical mechanism was preceded by hemolytic scission of the double bond, hemolytic rupture of the double bond which was highly improbable considering the initial polarization of the bond which was further improved under the field created by the electric double layer [37], [38].

4. Results and discussion

4.1. FTIR of GO and rGO

FTIR spectra for GO as show in Fig1a. It shows transmission peaks at 3446.56 cm^{-1} (O-H), with(C=O) at 1722.31 cm^{-1} (carbonyl/ carboxyl), (C=C) 1629.64 cm^{-1} (aromatic), (C-O) 1379 cm^{-1} (carboxy), (C-O) 1230.50 cm^{-1} (epoxy), (C-O) 1051.13 cm^{-1} (alkoxy) [39].

From FTIR spectra for rGO as shown in Fig. 2b. Carbonyl group peak (C=O) at 1722.3 is disappear and show peak at 1550.5 cm^{-1} belong to aromatic (C=C).

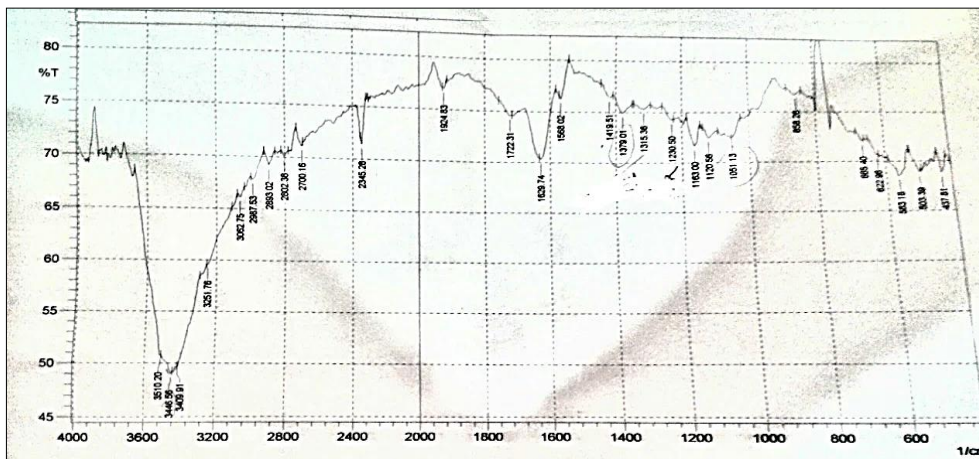


Fig. 1: A) FTIR For GO.

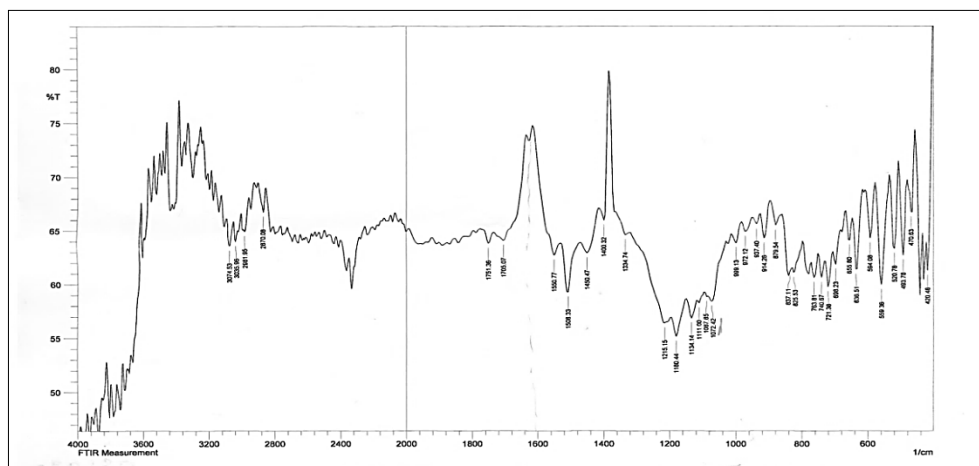


Fig. 1: B) FTIR for rGO.

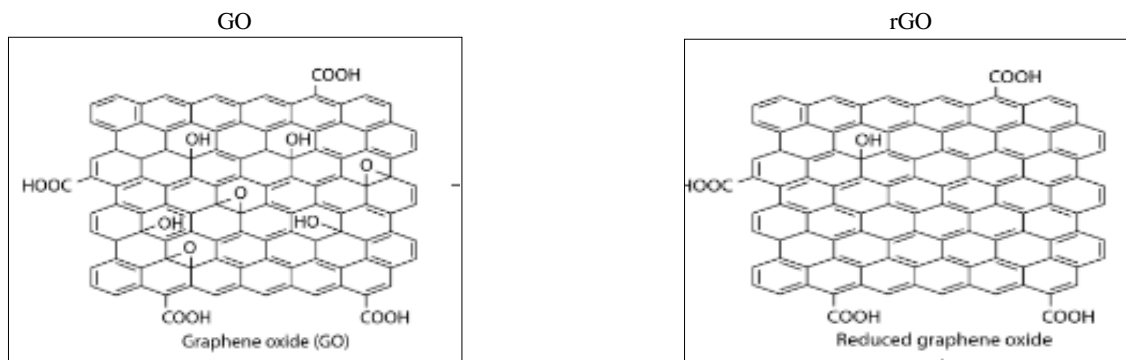


Fig. 2: Structure for GO and rGO [40].

Schematic structures of the GO and rGO represented according to the FTIR peaks as follow:

4.2. FTIR of NIP and PIP

FTIR spectra of NIP as shown in Fig. 3a. It shows peaks at 2543.93 cm^{-1} (O-H) of carboxylic acid, amide group (N-H) at 3514.06 cm^{-1} , with carbonyl group (C=O) of carboxylic acid at 1697 cm^{-1} , (C=C) at 1575.73 and 1562.23 cm^{-1} (aromatic), car-



bonyl group (C=O) of amide at 1640 cm^{-1} , (C=N) at 1600 cm^{-1} , aliphatic double bond (=CH) at 3141.82 cm^{-1} [41].

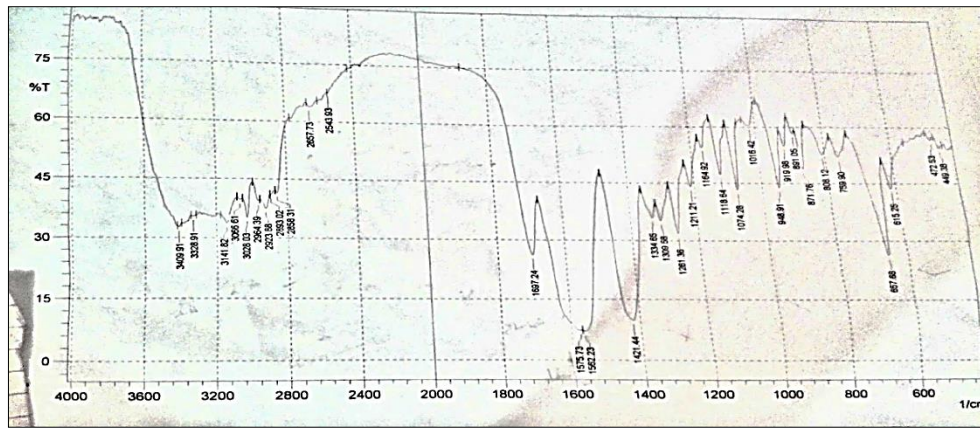


Fig. 3: A) FTIR Spectra for NIP.

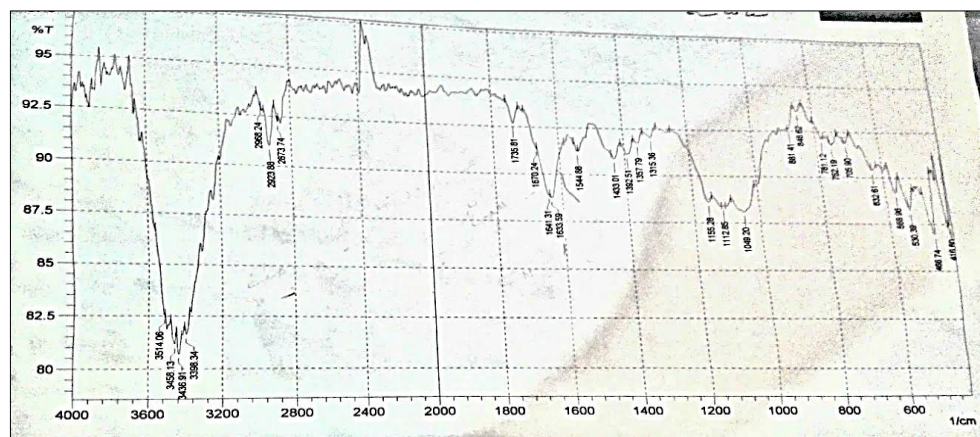


Fig. 3: B) FTIR Spectra for PIP.

FTIR spectra of PIP coating film on SS as shown in Fig. 3b. It shows peak of aliphatic double bond (=CH) at 3141.82 cm^{-1} was disappeared and confirm the formation of PIP.

4.3. Atomic force microscope (AFM)

Surface morphology of the S.S coated with polymeric coating (PIP) in absence and presence of ZnO_n and rGO were studied

through AFM technique [42]. AFM images were shown in (Fig.4a, 4b and 4c), for all coating layers. Show a degree of agglomeration of the nano materials due to adhesiveness of nano materials with polymer and the produced layer are higher density greater adhesive with larger particles.

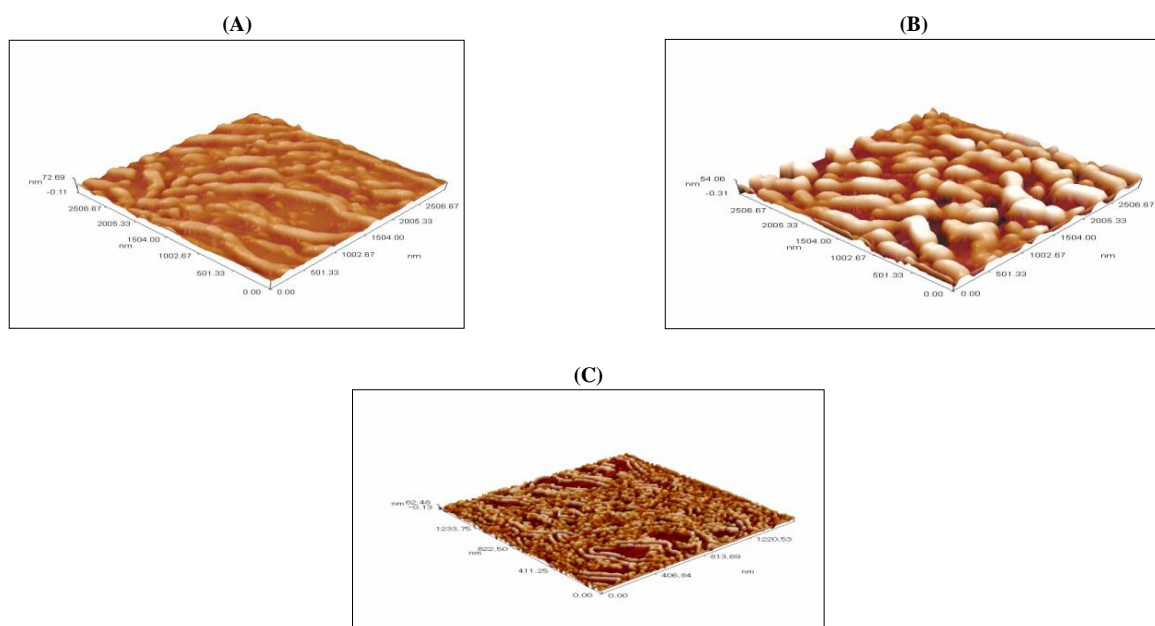


Fig. 4: A) PIP Coated on S.S, B) PIP Modified with rGO Coated on S.S, C) PIP Modified With ZnO_n Coated On S.S.

4.4. Corrosion measurements

The polarization resistance (R_p) was determined from Stern-Geary equation [43]:

$$R_p = b_{ac} b_{ca} / 2.303(b_{ac} + b_{ca}) i_{corr} \quad (1)$$

The cathodic (bc) and anodic (ba) Tafel slopes were determined from the slopes, the protection efficiency (PE %) calculated by the following equation [44]:

$$PE\% = (i_{corr})_{uncoated} - (i_{corr})_{coated} / (i_{corr})_{uncoated} \quad (2)$$

Where $(i_{corr})_{uncoated}$ and $(i_{corr})_{coated}$ were respectively the corrosion current densities of the uncoated and coated S.S, polarization curves for coated and uncoated S.S at 293 K represented in Fig.5.

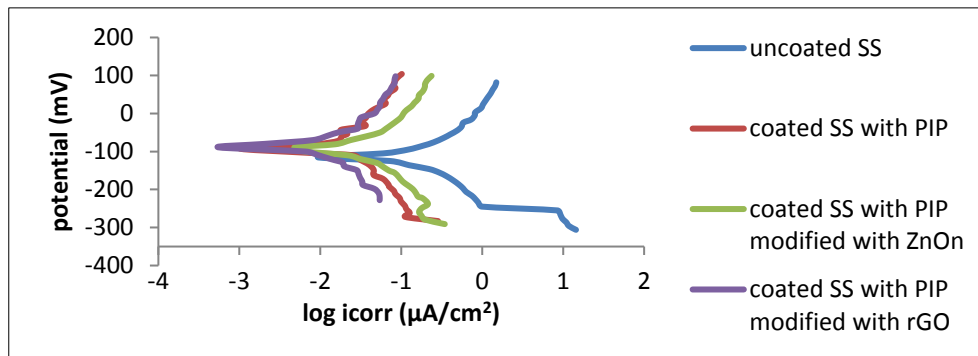


Fig. 5: Polarization Curves of S.S Coated by PIP and Modified PIP with Nanomaterials in 0.2 M HCl at 293K.

Table 1: Corrosion Parameters of S.S in 0.2M HCl for PIP and Modified PIP with Nanomaterials

Coating	T(K)	E_{corr} (mV)	i_{corr} ($\mu A/cm^2$)	-bc(mV/Dec)	ba(mV/Dec)	WL(g/m ² .d)	PL(mm/y)	$R_p \Omega.cm^2$	PE%
Uncoated S.S	293	113.5	43.27	48.5	47.1	3.48	0.471	239.786	-
	303	226	53.20	79.4	110.2	4.28	0.579	376.668	-
	313	235.4	56.77	149.0	120.7	4.57	0.618	510.035	-
	323	235.9	56.90	78.6	78.9	4.58	0.619	300.286	-
PIP	293	104.5	7.66	65.4	138.1	0.616	0.0833	2515.854	82.297
	303	104.6	13.63	119.8	206.8	1.10	0.148	2416.581	74.379
	313	187.3	15.07	126.4	236.5	1.22	0.164	2373.472	73.454
	323	230.2	15.28	129.9	219.3	1.23	0.166	2318.229	73.146
PIP modified with ZnO _n	293	86.6	6.06	79.9	91.9	0.487	0.066	3062.475	85.995
	303	92.9	7.85	89.5	97.3	0.632	0.085	2578.668	85.244
	313	93.3	11.03	128.9	140.9	0.888	0.120	2650.040	80.570
	323	98.2	13.56	148.2	149.3	1.09	0.147	2381.592	76.169
PIP modified with rGO	293	45.7	4.68	78.5	62.5	0.337	0.051	3228.425	89.184
	303	68.7	5.86	84.8	74.2	0.471	0.064	2932.318	88.985
	313	194.2	9.26	62.3	179.0	0.745	0.101	2167.099	83.689
	323	212.3	10.19	83.6	92.6	0.820	0.111	1872.161	82.091

These results shown in Table (1) reflect the following important facts, First: the E_{corr} shifted to the less negative values (more noble) at the same temperature after coating. Second: the corrosion current reduce after coated SS with PIP and PIP modified with nanomaterials. Third: polarization resistance (R_p) values were increased after coating.

4.5. Kinetic and thermodynamic of activation parameters

The effect of temperature on the protection efficiency for S.S corrosion in 0.2M HCl solution for coated and uncoated S.S by polymer with and without nanomaterials at temperature ranging (293-323K) wer expressed in term of activation parameters that involving E_a , A , ΔS^* , ΔG^* and ΔH^* . and these parameters were obtained from these equations [45]:

$$C.R = A \exp(-E_a/RT) \quad (3)$$

$$\log C.R = \log A - E_a / 2.303 RT \quad (4)$$

$$C.R = RT / Nh \exp(\Delta S^*/R) \exp(-\Delta H^*/RT) \quad (5)$$

$$(\log C.R/T) = \log R/Nh + \Delta S^*/2.303R - \Delta H^*/2.303RT \quad (6)$$

While the activation free energy ΔG^* was calculated using the following equation [46]

$$\Delta G^* = \Delta H^* - T\Delta S^* \quad (7)$$

Where, C.R is the corrosion rate, R the gas constant (8.315 J/K.mol), T the absolute temperature, A the pre exponential factor, h the Planks constant ($6.62 \cdot 10^{-34}$ J.S), N Avogadros number ($6.02 \cdot 10^{23}$), E_a the activation energy, ΔS^* the entropy of activation and ΔH^* the enthalpy of activation. The E_a and A values were obtained from slope and intercept respectively from the linear regression between $\log CR$ vs. $1/T$ as shown in Fig.6. While ΔH^* and ΔS^* were obtained from slope and intercept respectively from the linear regression between $\log CR/T$ vs. $1/T$ as shown in Fig.7.



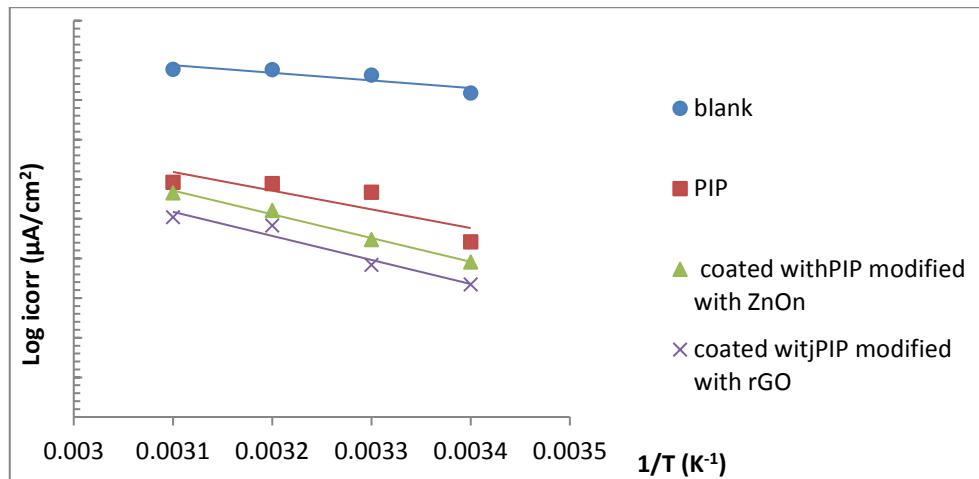


Fig. 6: Arrhenius Plot of Log C.R vs. 1/T in 0.2M Hcl for Coated and Uncoated S.S.

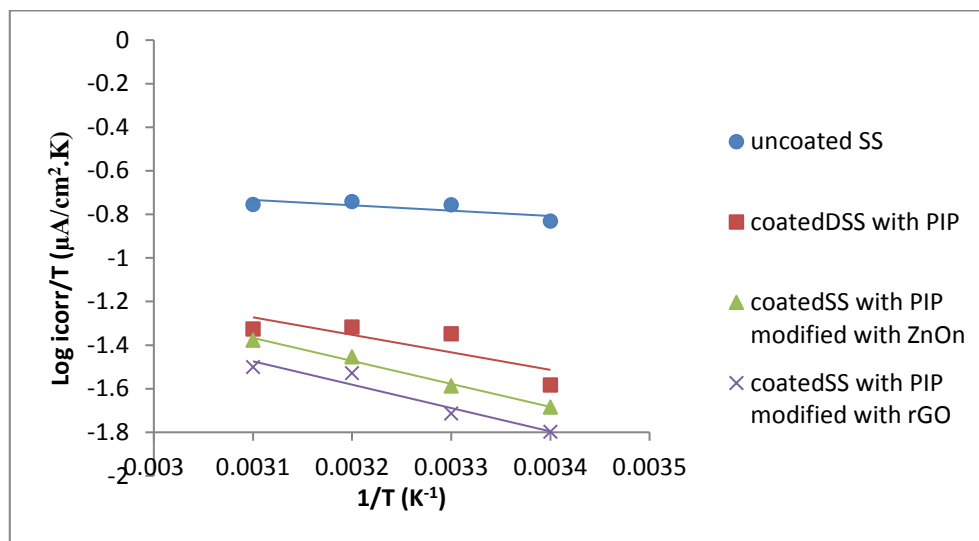


Fig. 7: Arrhenius Plot of Log C.R/T vs. 1/T in 0.2 M Hcl for Coated and Uncoated S.S.

Table 3: Activation Parameters for Coated and Uncoated S.S

coating	T(K)	ΔG^* (kJ/mol)	ΔH^* (kJ/mol)	$-\Delta S^*$ (J/mol.K)	R^2	E_a (kJ/mol)	A Molecule $s.cm^{-2}$.S ⁻¹	R^2
uncoated S.S	293	68.252	4.711	216.864	0.604	7.373	5.605×10^{26}	0.784
	303	70.421						
	313	72.589						
	323	74.758						
coated S.S with PIP	293	72.092	15.396	193.501	0.665	18.077	8.802×10^{27}	0.732
	303	74.027						
	313	75.962						
	323	77.897						
coated S.S with PIP modified with ZnO _n	293	73.036	20.203	180.317	0.99	22.941	4.326×10^{28}	0.992
	303	74.839						
	313	76.642						
	323	78.445						
coated S.S with PIP modified with rGO	293	73.664	20.547	181.303	0.933	23.228	3.759×10^{28}	0.946
	303	75.501						
	313	77.338						
	323	79.175						

The results were given in Table (3). The data illustrate that the thermodynamic activation functions (E_a & ΔH^*) of coated S.S were higher than those of uncoated S.S, also positive value of ΔH^* indicates to endothermic nature of transition state for coated and uncoated S.S, increase of ΔH^* values for the coated S.S reveals that corrosion rate is mainly controlled by kinetic parameters of activation [47]. The results of ΔS^* for uncoated and coated S.S were negative value, this refers that the activated complex in the rate determining step represents an association rather than dissolution step, meaning that, a decrease in disordering takes place on going from reactants to the activated complex [48]. The positive values of ΔG^* showed in Table (3) almost small change with

increasing temperature, and indicates to non-spontaneous nature of transition state for coated and uncoated S.S.

5. Conclusion

- 1) Electropolymerization of NIP on S.S was found to inhibit corrosion rate in 0.2 M HCl solution.
- 2) The corrosion current density (i_{corr}) and corrosion potential (E_{corr}) increased with increasing temperature.
- 3) The protection efficiency (PE %) of polymer increased after adding nanomaterials into monomer solution.

- 4) The protection efficiency (PE %) increased with decreasing temperature.
- 5) The thermodynamic activation functions (E_a and ΔH^*) for coated S.S were higher than those of the uncoated ones indicating higher energy barrier.
- 6) The entropy of activation ΔS^* for uncoated and coated SS were always negative. This indicates to decreases disordering takes place on going from reactants to the activated complex.

The positive values of ΔG^* were shown almost small changes with increasing temperature.

References

- [1] Waltman, R.J., Bargon, J., and Diaz, A.F., "Electrochemical studies of some conducting polythiophene films", *Journal of Physical Chemistry*, 87, pp: 1459-1463, 1983. <https://doi.org/10.1021/j100231a035>.
- [2] Sandeep C., "Graphene Oxide/Polyaniline Composites as Electrode Material for Supercapacitors", *Journal of Chemical and Pharmaceutical Research*, 9(4), pp: 285-291, 2017.
- [3] radilla Zapata, D. (2012), "Design, synthesis, characterization and development of novel organic conducting polymers with technological applications", in *Departament d'enginyeria química*, Universitat Politècnica de catalunya: Barcelona.
- [4] Chiarelli, P. A., Johal, M. S. Casson, J. L., Roberts, J. B., Robinson, J. M., and Wang, H. L. *Controlled Fabrication of Polyelectrolyte Multilayer Thin Films Using Spin-Assembly*, *Advanced Materials*, 13(15), pp: 1167-1171, 2001. [https://doi.org/10.1002/1521-4095\(200108\)13:15<1167::AID-ADMA1167>3.0.CO;2-A](https://doi.org/10.1002/1521-4095(200108)13:15<1167::AID-ADMA1167>3.0.CO;2-A).
- [6] Ulman, A. (1991) "An introduction to ultrathin organic films: from Langmuir-Blodgett to self-assembly", 127: Academic press New York.
- [7] Decher, G., Hong, J., and Schmitt, J., "Buildup of ultrathin multilayer films by a self-assembly process: III. Consecutively alternating adsorption of anionic and cationic polyelectrolytes on charged surfaces", *Thin solid films*, 210, pp: 831-835, 1992. [https://doi.org/10.1016/0040-6090\(92\)90417-A](https://doi.org/10.1016/0040-6090(92)90417-A).
- [8] Decher, G., "Fuzzy nanoassemblies: toward layered polymeric multicomposites. *Science*", 277(5330), pp: 1232-1237, 1997. <https://doi.org/10.1126/science.277.5330.1232>.
- [9] Bertrand, P. Jonas, A., Laschewsky, A., and Legras, R., "Ultrathin polymer coatings by complexation of polyelectrolytes at interfaces: suitable materials, structure and properties", *Macromolecular Rapid Communications*, 21(7) pp:319-348, 2000. [https://doi.org/10.1002/\(SICI\)1521-3927\(20000401\)21:7<319::AID-MARC319>3.0.CO;2-7](https://doi.org/10.1002/(SICI)1521-3927(20000401)21:7<319::AID-MARC319>3.0.CO;2-7).
- [10] Hammond, P. T., "Recent explorations in electrostatic multilayer thin film assembly", *Current Opinion in Colloid & Interface Science*, 4(6) pp: 430-442, 1999. [https://doi.org/10.1016/S1359-0294\(00\)00022-4](https://doi.org/10.1016/S1359-0294(00)00022-4).
- [11] Hammond, P. T., "Form and function in multilayer assembly: new applications at the nanoscale". *Advanced Materials*, 16(15) pp: 1271-1293, 2004. <https://doi.org/10.1002/adma.200400760>.
- [12] Holder, E., Tessler, N. and Rogach, A. L., "Hybrid nanocomposite materials with organic and inorganic components for optoelectronic devices", *Journal of Materials Chemistry*, 18(10) pp: 1064-1078, 2008. <https://doi.org/10.1039/b712176h>.
- [13] Joanny, J. "Polyelectrolyte adsorption and charge inversion.", *The European Physical Journal B-Condensed Matter and Complex Systems*, 9(1) pp: 117-122, 1999. <https://doi.org/10.1007/s100510050747>.
- [14] Qin, X., Wang, H. Wang, X., Miao, Z., Chen, L., Zhao, W., Shan, M., and Chen, Q. "Amperometric biosensors based on gold nanoparticles-decorated multiwalled carbon nanotubes-poly(diallyldimethylammonium chloride) biocomposite for the determination of choline". *Sensors and Actuators B: Chemical*, 147(2), pp: 593-598, 2010. <https://doi.org/10.1016/j.snb.2010.03.010>.
- [15] Steitz, R., Jaeger, W., and Klitzing, R. v. "Influence of charge density and ionic strength on the multilayer formation of strong polyelectrolytes". *Langmuir*, 17(15), pp: 4471-4474, 2001. <https://doi.org/10.1021/la010168d>.
- [16] Dubas, S. T. and Schlenoff, J. B. "Swelling and smoothing of polyelectrolyte multilayers by salt". *Langmuir*, 17(25) pp: 7725-7727, 2001. <https://doi.org/10.1021/la0112099>.
- [17] Blomberg, E., Poptoshev, E., Claesson, P. M., and Caruso, F. "Surface interactions during polyelectrolyte multilayer buildup. 1. Interactions and layer structure in dilute electrolyte solutions". *Langmuir*, 20(13), pp: 5432-5438, 2004. <https://doi.org/10.1021/la049636k>.
- [18] Guo, Y., Geng, W., and Sun, J. "Layer-by-Layer Deposition of Polyelectrolyte-Polyelectrolyte Complexes for Multilayer Film Fabrication". *Langmuir*, 25(2) pp: 1004-1010, 2008. <https://doi.org/10.1021/la803479a>.
- [19] Ladam, G., Schaad, P., Voegel, J., Schaaf, P., Decher, G., and Cuisinier, F. "In situ determination of the structural properties of initially deposited polyelectrolyte multilayers". *Langmuir*, 16(3), pp: 1249-1255, 2000. <https://doi.org/10.1021/la990650k>.
- [20] Klitzing, R. v. "Internal structure of polyelectrolyte multilayer assemblies". *Physical Chemistry Chemical Physics*, 8(43) pp: 5012-5033, 2006. <https://doi.org/10.1039/b607760a>.
- [21] Elzbiaciak, M., Zapotoczny, S., Nowak, P., Krastev, R., Nowakowska, M., and Warszynski, P. "Influence of pH on the structure of multilayer films composed of strong and weak polyelectrolytes". *Langmuir*, 25(5), pp: 3255-3259, 2009. <https://doi.org/10.1021/la803988k>.
- [22] Kolasińska, M. and Warszyński, P. "The effect of nature of polyions and treatment after deposition on wetting characteristics of polyelectrolyte multilayers". *Applied surface science*, 252(3), pp: 759-765, 2005. <https://doi.org/10.1016/j.apsusc.2005.02.060>.
- [23] Tong, Bohm and Song M. "Carbon Based Coating on Steel with Improved Electrical Conductivity, Austin J Nanomed Nanotechnol 3(1): id1041): pp: 1-7, 2015.
- [24] Potts, J. R., Shankar, O., Du, L. and Ruoff, R. S. "Processing morphology property relationships and composite theory analysis of reduced graphene oxide/natural rubber nanocomposites". *Macromolecules*, 45(1), pp: 6045-6055, 2012. <https://doi.org/10.1021/ma300706k>.
- [25] Chang, C. H., Tsao, C. H., Chih, W. P., Tzu, C. Y., Hsin, I. L., Wei, I. H., Chang, J. W., Ta, I. Y. and Jui, M. Y. "Novel anticorrosion coatings prepared from polyaniline/graphene composites. *Carbon*", 50, pp: 5044-5051, 2012. <https://doi.org/10.1016/j.carbon.2012.06.043>.
- [26] Kung, C. C., Min, H. H., Hsin, I. L., Mei, C. L., Pei, J. L., Chien, H. H., Wei, F. J., Tsao, L. C., Yen, W., Jui, M. Y. and Wei, R. "Room temperature cured hydrophobic epoxy/graphene composites as a corrosion inhibitor for cold-rolled steel". *Carbon*, 66, pp: 144-153, 2014. <https://doi.org/10.1016/j.carbon.2013.08.052>.
- [27] Xiao, H., Zongyou, Y., Shixin, W., Xiaoying, Q., Qiyuan, H., Qichun, Z., Qingyu, Y., Freddy, B. and Hua Z. "Graphene-based materials: synthesis, characterization, properties, and applications". *Small*, 7(14), pp: 1876-1902, 2011. <https://doi.org/10.1002/sml.201002009>.
- [28] Zhiyi, Z., Wenhui, Z., Diansen, L., Youyi, S., Zhuo, W., Chunling, H., Lu C., Yang, C. and Yaqing, L. "Mechanical and anticorrosive properties of graphene/epoxy resin composites coating prepared by in-situ method". *International J. Molecular Science*, 16(1), pp: 2239-2251, 2015. <https://doi.org/10.3390/ijms16012239>.
- [29] William, S. H. Jr. and Richard, E. O. "Preparation of graphitic oxide". *Journal of American Chemical Society*, 80, pp: 1339-1394, 1958. <https://doi.org/10.1021/ja01539a017>.
- [30] Khulood, A.S. Khalil, S.K, and Muna, I.K. "Preparation of poly(N-imidazolylmaleamic acid)/nanomaterial coating films on stainless steel by electrochemical polymerization to study the anticorrosion and antibacterial action". *Journal of Pharmacy and Biological Sciences*, 13, PP: 30-36, 2018.
- [31] Younang, E., Léonard-Stibbe, E., Viel, P., Defranceschi, M., Lécayon, G., and Delhalle J. "Prospective theoretical and experimental study towards electrochemically grafted poly(N-vinyl-2-pyrrolidone) films on metallic surfaces". *Molec. Engin.* 1(4), pp: 317-332, 1992. <https://doi.org/10.1007/BF00176804>.
- [32] Léonard-Stibbe, E., Lécayon, G., Deniau, G., Viel, P., Defranceschi, M., Legeay, G., and Delhalle J. "The cationic polymerization of N-vinyl-2-pyrrolidone initiated electrochemically by anodic polarization on a Pt surface", *J. Polym. Sci.: Part A, Polym. Chem.*, 32(8), pp: 1551-1555, 1994. <https://doi.org/10.1002/pola.1994.080320816>.
- [33] Je'ro'me, R.; and Mertens, M. "The Electrochemical Polymerization of Acrylonitrile and N-Vinylpyrrolidone" *New Insight into the Mechanism, L. Adv. Mater.*, 7(9), pp: 807-809, 1995. <https://doi.org/10.1002/adma.19950070911>.
- [34] Beamson, G., and Briggs, D. "High Resolution XPS of Organic Polymers", John Wiley & Sons: Chichester, pp: 192, 1992.

- [35] Ivanov, D.V. "Chemical-Sensitivity of the Thickness-Shear-Mode Quartz-Resonator Nanobalance", A. J. Electrochem. Soc., 143(9), pp: 2835-2841, 1996. <https://doi.org/10.1149/1.1837115>.
- [36] Czerwinski, W. K. "Solvent effects on free-radical polymerization, 2. IR and NMR spectroscopic analysis of monomer mixtures of methyl methacrylate and N-vinyl-2-pyrrolidone in bulk and in model solvents", Chem., 192(6), pp: 1297-1305, 1991.
- [37] Lin-Vien, D., Colthup, N. B., Fateley, W. G., and Grasselli, J. G. "The Handbook of Infrared and Raman Characteristic Frequencies of Organic Molecules", Academic: San Diego, pp: 74, 1991.
- [38] Mertens, M., Calberg, C., Martinot, L., and Jérôme, R. "The Electroreduction of Acrylonitrile - A New Insight into the Mechanism", Macromolecules, 29(14), pp: 4910-4918, 1996. <https://doi.org/10.1021/ma946442a>.
- [39] Raynaud, M., Reynaud, C., Ellinger, Y., Hennico, G., and Delhalle, J. "High Electric-Field Effects on the Acrylonitrile Molecule - an Abinitio Study", J. Chem. Phys., 142(2), pp:191-201, 1990.
- [40] Devesh K. M., Subhendu B., Mostafaizur R., and Dipak K. "Morphology and Cyclic Voltammetry Analysis of in situ Polymerized Polyaniline /Graphene Composites" J. Electrochem. Sci.Eng., 3 (4), pp:157-166, 2015.
- [41] Sasha, S. , Dmitriy, A.D., Richard, D. P., Kevin, A. K., Alfred, K., Yuanyuan, J., Yue, W. , Sonbinh, T. N. and Rodney, S. R." Synthesis of graphene-based nanosheets via chemical reduction of exfoliated graphite oxide". Carbon, 45, pp: 1558-1565, 2007. <https://doi.org/10.1016/j.carbon.2007.02.034>.
- [42] Silverstein R.M., Webster, F.X., and Kiemle, D.J. (1963). "Spectrometric Identification of Organic Compounds", 7th ed., John Wiley & Sons, Westford, US.
- [43] Quraishi M. and Sudhish K., "Poly (aniline-formaldehyde): A new and effective corrosion inhibitor for mild steel in hydrochloric acid", Materials Chemistry and Physics, 113, pp: 685-689, 2009. <https://doi.org/10.1016/j.matchemphys.2008.08.028>.
- [44] Jalal M. and Yousif K., Bulletin of the Chemical Society of Japan, 62, (1989), pp: 1237. <https://doi.org/10.1246/bcsj.62.1237>.
- [45] Trethewey, K.R., and Chamberlain, J. (1996). "Corrosion for Science and Engineering", 2nd, Addition Wesley Longman Ltd.
- [46] Frankel, G.S., Stockert, L., Hunkeler, F., and Boehni, H. "Pitting corrosion", 43, pp:429, 1987.
- [47] Fontana, M. G. (1987) "Corrosion Engineering." 3rd ed. McGraw-Hill. 3., New York.
- [48] Hellmann, R. and Tisserand, D." Dissolution kinetics as a function of the Gibbs free energy of reaction: An experimental study based on albite feldspar". Geochimica et Cosmochimica Acta, 70(2), pp: 364-383, 2006. <https://doi.org/10.1016/j.gca.2005.10.007>.
- [49] Gomma, M. and Wahdan, M. "Corrosion behavior of Zn in alcohol-water solvents". Mater. Chem. Phys, 39, pp: 193, 1995.